

# Efficient Decision Feedback Equalization for Sparse Wireless Channels

Athanasios A. Rontogiannis, *Member, IEEE*, and Kostas Berberidis, *Member, IEEE*

**Abstract**—In this paper, a new efficient decision feedback equalizer (DFE) appropriate for channels with long and sparse impulse response (IR) is proposed. Such channels are encountered in many high-speed wireless communications applications. It is shown that, in cases of sparse channels, the feedforward and feedback (FB) filters of the DFE have a particular structure, which can be exploited to derive efficient implementations of the DFE, provided that the time delays of the channel IR multipath components are known. This latter task is accomplished by a novel technique, which estimates the time delays based on the form of the channel input-output cross-correlation sequence in the frequency domain. A distinct feature of the resulting DFE is that the involved FB filter consists of a reduced number of active taps. As a result, it exhibits considerable computational savings, faster convergence, and improved tracking capabilities as compared with the conventional DFE. Note that faster convergence implies that a shorter training sequence is required. Moreover, the new algorithm has a simple form and its steady-state performance is almost identical to that of the conventional DFE.

**Index Terms**—Adaptive equalizers, decision feedback equalizers (DFEs), multipath channels.

## I. INTRODUCTION

IN MANY wireless communication systems the involved multipath channels exhibit a long time dispersion, and delay spreads of up to 40  $\mu$ s are often encountered. A typical application of this is high definition television (HDTV) signal terrestrial transmission, where the involved channels consist of a few nonnegligible echoes, some of which may have quite large time delays with respect to the main signal (see for instance the HDTV test channels reported in several ATSC documents<sup>1</sup> and summarized in [17]). If the information signal is transmitted at high symbol rates through such a dispersive channel, then the introduced intersymbol interference (ISI) has a span of several tens up to hundreds of symbol intervals. This in turn implies that quite long adaptive equalizers are required at the receiver's end in order to reduce effectively the ISI component of the received signal. Note that the situation is even more demanding whenever the channel frequency response exhibits deep nulls.

Manuscript received August 6, 2001; revised June 31, 2002; accepted August 2, 2002. The editor coordinating the review of this paper and approving it for publication is D. Goeckel.

A. A. Rontogiannis is with Information Processing Laboratory, School of Natural Resources Management, University of Ioannina, 30100 Agrinio, Greece (e-mail: arontogi@cc.uoi.gr).

K. Berberidis is with the Department of Computer Engineering and Informatics, School of Engineering, University of Patras, 26500 Rio-Patras, Greece (e-mail: berberid@ceid.upatras.gr).

Digital Object Identifier 10.1109/TWC.2003.811189

<sup>1</sup>The relevant documents can be found at the Web site of ATSC (Advanced Television Standards Committee), <http://www.atsc.org>.

The adaptive decision feedback equalizer (DFE) has been widely accepted as an effective technique for reducing ISI [1], [2]. Moreover, it has been shown that the DFE structure is particularly suitable for multipath channels, since most part of ISI is due to the long postcursor portion of the impulse response (IR) (see, for instance, [7]). Recall that an important feature of the DFE is that the postcursor ISI is almost perfectly cancelled by the feedback (FB) filter, provided of course that the previous decisions are correct. Since the postcursor ISI is cancelled by the FB filter, a relatively shorter feedforward (FF) filter is adequate to reduce the remaining ISI. Moreover since noise is involved only in the output of the FF filter, the DFE exhibits less noise enhancement effects as compared with linear equalizers. In high-speed wireless applications, of the type described above, the implementation of a DFE algorithm becomes a difficult task for two main reasons. First, due to the small intersymbol interval, the time available for real-time computations is very limited. Second, due to the long span of the introduced ISI, the DFE must have a large number of taps, which implies heavy computational load per iteration.

During the last decade there have been many efforts in different directions toward developing efficient implementations of the DFE. As such directions, we mention IIR methods, block adaptive implementations, efficient algebraic solutions, modified DFE schemes, etc. [4]–[12]. As mentioned above, in the applications of interest, the involved multipath channel has a discrete sparse form. Efficient DFE schemes which exploit the sparseness of the channel IR have been derived in [13]–[15]. In [13], the performance of the modified DFE algorithm proposed in [11] is improved by properly selecting a small number of FF taps based on output signal-to-noise ratio (SNR) measures. In [14], two DFE algorithms are proposed whose FF and FB filters are obtained based on the approach described in [10]. This is done after the channel IR coefficients have been estimated using least squares (LS). Reduction in complexity is achieved due to the small size (or absence) of the FB filter and a proper selection of a limited number of IR and FB coefficients. Note that LS channel estimation and FF, FB filter taps computation is done on a periodic basis. A similar approach, in which instead of LS, a matching pursuit method is used for estimating the channel IR coefficients, is derived in [15].

In this paper, a new DFE algorithm, appropriate for sparse multipath channels is derived. The algorithm consists of two steps. In the first step, the time delays of the multipath components are estimated in a novel way by properly exploiting the channel IR form [16]. In the second step, the DFE is applied, with the FB filter having a significantly reduced number of taps. These taps are selected so as to act only on time positions

associated with the estimated time delays of the involved multipath components. A distinct feature of the novel approach followed in this paper is that the required channel parameters are the locations of the multipath components. This is opposed to most of the existing works [14], [15], in which the whole channel IR has to be initially estimated. Moreover, the relation between the active FB tap positions and the echo time delays is determined by investigating the special structure of the FF and FB filters in cases of sparse channels.

The main advantages of this algorithm with respect to the conventional DFE are its lower complexity, faster convergence, and improved tracking capabilities. It is important to note that due to the faster convergence the proposed algorithm requires a shorter training sequence as compared with classical DFE, thus, it offers an additional saving in bandwidth. Note that its overall complexity is of the order of the number of multipath components and hence it is, in practice, several times lower as compared with the conventional DFE.

The paper is outlined as follows. In Section II, the multipath channel is described and the problem is formulated. In Section III, the proposed efficient method for estimating and tracking the time delays is presented. The new DFE algorithm is developed in Section IV and relevant computational issues are discussed. In Section V, the new algorithm is tested and some indicative experimental results are provided. Section VI concludes the work.

## II. PROBLEM FORMULATION

In this section, we first formulate the problem of information transmission through a multipath channel, and we recall the conventional and well-studied DFE structure which is our starting point for the derivation of the new equalization technique. The notation used throughout the paper is as follows.  $x(n)$  denotes a scalar sample or symbol of sequence  $\{x\}$  at time  $n$ ,  $c_i(n)$  is the  $i$ th coefficient of filter  $c$  at time  $n$ , and  $X(k)$  is the  $k$ th frequency bin of the discrete Fourier transform (DFT) of a sequence related to  $\{x\}$ . Finally, vectors and matrices are denoted as lower case bold roman type and as upper case slanted, respectively.

### A. Baseband Multipath Channel

The multipath channel is encountered in almost all wireless communication systems, however, its particular form is highly dependent on the specific system and the application environment (i.e., bit rate, modulation type, carrier frequency, transmitter–receiver separation and the around topography, cell type—if it is for a cellular system—and the receiver’s motion within the cell, etc.).

In general, the baseband IR of a multipath channel with discrete components is written as [2]

$$h_c(t, \tau) = \sum_i \alpha_i(t, \tau) e^{j(2\pi f_c \tau_i(t) + \phi_i(t, \tau))} \delta(\tau - \tau_i(t)) \quad (1)$$

where  $\alpha_i(t, \tau)$ ,  $\tau_i(t)$  are the real amplitudes and excess delays, respectively, of the  $i$ th multipath component at time  $t$ . The phase term  $2\pi f_c \tau_i(t) + \phi_i(t, \tau)$  represents the phase shift due to free

space propagation of the  $i$ th multipath component, plus any additional phase shifts which are encountered in the channel. If the channel IR is assumed to be invariant within a small-scale time interval, then (1) can be simplified to

$$h_c(\tau) = \sum_i \alpha_i e^{-j\theta_i} \delta(\tau - \tau_i). \quad (2)$$

The overall channel IR, including the combined transmitter and receiver filters’ response, say  $p(\tau)$ , can be written as

$$h(\tau) = \sum_i \alpha_i e^{-j\theta_i} p(\tau - \tau_i). \quad (3)$$

As mentioned in the introduction, in this paper, we deal with sparse multipath channels having a relatively long IR. Due to the sparseness of the multipath channel IR and the form of the pulse shaping function  $p(\tau)$ , which decreases rapidly, the overall symbol spaced channel IR remains sparse and can be expressed as<sup>2</sup>

$$h(nT) = \sum_{l=0}^L h_{n_l} \delta(nT - n_l T) \quad (4)$$

where  $L + 1$  is the number of the dominant IR components appearing at the symbol spaced time instants,  $h_{n_l}$  is the complex amplitude of the  $l$ th component, and  $n_l T$  its respective delay, with  $T$  being the symbol period. Delay  $n_0$  corresponds to the main signal<sup>3</sup> ( $n_0 = 0$ ), while the remaining ones correspond either to causal ( $n_l > 0$ ) or to anticausal ( $n_l < 0$ ) components. The symbol spaced IR spans  $k_1$  precursor and  $k_2$  postcursor symbols, respectively. That is the symbol spaced channel IR can be written in the vector form

$$\mathbf{h} = [h_{-k_1} \ \cdots \ h_0 \ \cdots \ h_{k_2}]^T. \quad (5)$$

From the total of the  $(k_1 + k_2 + 1)$  IR coefficients only  $L + 1$  are assumed to be nonnegligible, located at the  $n_l$  positions.

### B. Conventional DFE

Taking into account (4), the sampled output of the multipath channel can be written as follows:

$$x(n) = \sum_{l=0}^L h_{n_l} u(n - n_l) + w(n) \quad (6)$$

where  $\{u\}$  is an independent identically distributed (i.i.d.) symbol sequence with variance  $\sigma_u^2$  and  $\{w\}$  is zero-mean complex white Gaussian noise uncorrelated with the input sequence, with variance  $\sigma_w^2$ . Note that symbol period  $T$  has been omitted for reasons of simplicity. Obviously,  $\{x\}$  suffers from intersymbol interference due to the presence of undesired multipath components and in most cases equalization is necessary for reliable reception.

<sup>2</sup>It is readily understood that for each multipath component  $i$  in (2), the number of significant components in the symbol spaced model (4) is small, depending on the delay  $\tau_i$ . All other components can be considered negligible.

<sup>3</sup>Correct timing information is assumed.

As mentioned in the introduction, the DFE structure is particularly suitable for equalizing multipath channels. The LMS-based adaptive DFE is given by the following set of equations:

$$\hat{u}(n) = \sum_{k=-M+1}^0 c_k(n)x(n-k) + \sum_{k=1}^N b_k(n)\tilde{u}(n-k) \quad (7)$$

$$\tilde{u}(n) = f\{\hat{u}(n)\} \quad (8)$$

$$e(n) = \hat{u}(n) - \tilde{u}(n) \quad (9)$$

$$c_k(n+1) = c_k(n) - 2\mu^c x^*(n-k)e(n) \quad (10)$$

$$k = -M+1, \dots, 0$$

$$b_k(n+1) = b_k(n) - 2\mu^b \tilde{u}^*(n-k)e(n) \quad (11)$$

$$k = 1, \dots, N$$

where  $\{x\}$  and  $\{\tilde{u}\}$  denote the equalizer's input and decision sequences, respectively,  $c_k$  are the coefficients of the  $M$ -length FF filter, and  $b_k$  are the coefficients of the  $N$ -length FB filter ( $N$  is taken at least equal to the channel span [10]).  $f\{\cdot\}$  stands for the decision device function,  $\mu^c$ ,  $\mu^b$ , are the step sizes and  $*$  denotes complex conjugation. It is assumed that a training sequence of appropriate length is available ensuring convergence of the equalizer. That is the equalizer operates initially in a training mode and then switches to a decision directed mode. In the following sections, first, a frequency domain procedure is proposed for detecting the time delays of the multipath components of the channel IR. Then, a new efficient DFE structure is derived, which takes advantage of the special properties of the multipath channel.

### III. ESTIMATION OF THE ECHO DELAYS

A well-established nonparametric procedure for estimating the time delays of the multipath components is based on a proper cross-correlation of the input symbols with the corresponding channel output samples. In a time domain implementation, the estimation of the cross-correlation sequence for  $N$  lags requires  $O(N)$  operations per sample. It is shown that, an appropriate frequency domain expression of the cross-correlation sequence can be viewed as a sum of complex harmonics, with the unknown time delays interpreted as frequencies. Thus, to estimate the time delays, we suggest an FFT-based scheme of complexity  $\log(N)$  per sample. The proposed scheme stems from an appropriate partitioning of both channel input and output sequences and is described below.

Let us first formulate the following  $2N$ -DFT sequences for  $k = 0, 1, \dots, 2N-1$ :

$$U(k) = \sum_{m=p}^{N+p-1} u(n+m)e^{-j(2\pi/2N)mk} \quad (12)$$

$$X(k) = \sum_{i=0}^{2N-1} x(n+i)e^{-j(2\pi/2N)ik} \quad (13)$$

where  $p$  is assumed to be an overestimated value of the noncausal size of the channel IR (i.e.,  $p > k_1$ ). The same is presumed for the quantity  $N-p$  as far as the size of the causal part of the channel IR is concerned. If these facts hold true, the method which is described below detects the positions of all

precursor and postcursor components. Note that  $X(k)$  in (13) is based on a  $2N$ -length output sequence, while  $U(k)$  in (12) results from an  $N$ -length input sequence padded with  $N$  zeros. As it will become evident from the subsequent derivation, this is done in order for all samples of the cross-correlation sequence to be equally weighted. Indeed, if we consider the expected value of the product of the above sequences, we obtain

$$\mathcal{E}\{X(k)U^*(k)\} = \sum_{i=0}^{2N-1} \sum_{m=p}^{N+p-1} \mathcal{E}\{x(n+i)u^*(n+m)\}e^{-j(\pi/N)(i-m)k} \quad (14)$$

where  $\mathcal{E}\{\cdot\}$  denotes the expectation operator.<sup>4</sup> If we now substitute (6) to (14), we get

$$\mathcal{E}\{X(k)U^*(k)\} = \sum_{l=0}^L h_{nl} \sum_{i=0}^{2N-1} \sum_{m=p}^{N+p-1} \mathcal{E}\{u(n+i-n_l)u^*(n+m)\}e^{-j(\pi/N)(i-m)k}. \quad (15)$$

Since  $p$  is larger than the noncausal part of the channel IR, it is easily shown that for every  $l$  the indices of  $u$  and  $u^*$  in (15) are identical for  $N$  combinations of  $m$  and  $i$  (with  $m = i - n_l$ ). Therefore, due to the i.i.d. property of the input sequence (15) is written as

$$\mathcal{E}\{X(k)U^*(k)\} = N\sigma_u^2 \sum_{l=0}^L h_{nl} e^{-j(\pi/N)n_l k} \quad (16)$$

for  $k = 0, 1, \dots, 2N-1$ . That is, we end up with a sum of complex harmonics at normalized frequencies  $n_l/2N$ . Applying the  $2N$ -IDFT to the resulting sequence, the locations  $n_l$  of the multipath components are determined at the nonnegligible points of the IDFT.

Obviously, in a practical situation, time averaging is used instead of  $\mathcal{E}\{\cdot\}$  in order to implement (16). In cases where the channel is assumed stationary, the above procedure can be done once during the training phase and then the obtained time delays can be used in the algorithm as described in the next section. Of course, in most situations in practice, the channel exhibits variations and, thus, the required time delays have to be tracked continuously. During tracking, the frequency domain expression of the cross-correlation sequence is formed using the decisions provided by the equalizer (which operates in a decision directed mode).

Exponentially fading memory is imposed on the estimation procedure by including a forgetting factor  $\lambda$  in the frequency domain expression of the cross-correlation sequence as follows:

$$C_{UX}^{(R)}(k) = \sum_{r=0}^{R-1} \lambda^{(R-1-r)N} X_r(k)U_r^*(k) \quad (17)$$

<sup>4</sup>Note that  $\mathcal{E}\{X(k)U^*(k)\}$  is related to the input-output cross-spectrum power density. Specifically, it is easily shown that the  $2N$ -IDFT of this quantity contains the cross-correlation coefficients of lags  $-p, -p+1, \dots, N-p-1$ .

where  $0 \ll \lambda < 1$  and

$$\begin{aligned} X_r(k) &= \sum_{i=0}^{2N-1} x(n+rN+i)e^{-j(2\pi/2N)ik} \\ U_r(k) &= \sum_{m=p}^{N+p-1} \lambda^{N+p-m-1} u(n+rN+m)e^{-j(2\pi/2N)mk} \end{aligned} \quad (18)$$

for  $k = 0, 1, \dots, 2N - 1$ . Note that if factor  $\lambda$  were included only in (17), then the exponential weighting would be applied on a block-by-block basis, thus affecting the tracking capabilities of the new algorithms. However, additionally including  $\lambda$  in (18) is equivalent to applying an exponential window in the time-domain sample-by-sample computation of the cross-correlation lags. When a new  $N$ -length block of input and output samples is available,  $C_{UX}^{(R)}(k)$  is updated as

$$\begin{aligned} C_{UX}^{(R+1)}(k) &= \lambda^N C_{UX}^{(R)}(k) + X_R(k)U_R^*(k) \\ k &= 0, 1, \dots, 2N - 1. \end{aligned} \quad (19)$$

Recall that quantity  $C_{UX}^R(k)$  can be interpreted as a sum of complex harmonics with unknown frequencies and complex amplitudes. Indeed, as can be easily seen by inspecting (16), the frequency bin  $k$  corresponds to the sequence index while the time delay  $n_l$  corresponds to the unknown frequency. This particular form is encountered in many signal processing applications (e.g., harmonic retrieval, direction of arrivals estimation, etc.). There are many well-established techniques proposed in the literature to extract the unknown parameters of the harmonic components [20]. For instance, an efficient parametric technique is based on modeling  $C_{UX}^R(k)$  as an autoregressive process of order  $m > L + 1$ . This technique, adapted to our case, has been tested and found that it requires almost 50% less training symbols in order to yield an initial reliable estimate of the time delays as compared with the nonparametric FFT-based technique in this section. Also, the parametric technique has a better performance in resolving closely spaced time delays. Of course this improved performance is offered at the expense of an increased complexity.

An alternative approach is to use a blind [18] or semiblind [19] method for the estimation of the channel time delays and amplitudes. The advantage of such an approach is that the number of training symbols for the estimation of the channel echoes is nullified or significantly reduced. The main drawback is the increase in computational and implementation complexity, especially when the method is to be used in a time varying environment. The use of an efficient high resolution, blind or semiblind technique in the problem of interest, without affecting significantly the overall complexity, is a subject under current investigation.

*Determination of Dominant Components:* We see from (17) that  $R \cdot N$  samples of  $\{u\}$  and  $\{x\}$  are used to compute  $C_{UX}^{(R)}(k)$ . The  $L + 1$  IDFT points of (17) having the highest amplitude are then chosen as the desired locations. The number  $L$  of the dominant undesired components can be preset by the designer by taking into account a worst case scenario for the specific application. Alternatively, number  $L$  can be computed from the data

using rank determination techniques. Another strategy would be to set a threshold and select the locations of the IDFT points of (17) having amplitudes which exceed this threshold.

#### IV. THE NEW METHOD

In the proposed algorithm, we focus our attention to the demanding FB part and reduce the computational load by properly selecting  $O(L)$  number of taps out of  $N$  taps. The main idea behind the derivation of the algorithm is that due to the channel sparseness, the FB filter also possesses a specific sparse form. After exploiting its sparse form, the FB filter is built so as to act only to a restricted set of tap positions. As a result, the algorithm offers significant computational savings while its steady-state error performance is similar to that of the conventional DFE.

In the initial stage of the algorithm, the method described in the previous section, is used for an adequate number of blocks  $R = R_0$  and the time delays  $n_l$  are estimated. Such an approach introduces a delay to the algorithm which increases as the number of blocks  $R_0$  increases. However, the greater the parameter  $R_0$ , the higher is the degree of accuracy in selecting the correct positions. As it will be shown below, the initial delay of the algorithm is fully compensated by the fast convergence achieved by the new DFE scheme.

##### A. Derivation of the Algorithm

It is well known [1], [3] that in the minimum mean-squared error (MMSE) DFE, the FF and FB coefficients can be expressed in terms of the channel IR coefficients. Indeed, based on the assumption that previously detected symbols are correct, the minimization of the mean-squared error (MSE)  $\mathcal{E}\{|e(n)|^2\}$  leads to the following set of equations for the FF filter  $\mathbf{c}_M$  and the FB filter  $\mathbf{b}_N$ <sup>5</sup>

$$\mathbf{c}_M = \left( H_1 H_1^H + \frac{\sigma_w^2}{\sigma_u^2} I_M \right)^{-1} H_1 \mathbf{e}_{M+k_1} \quad (20)$$

$$\mathbf{b}_N = \begin{bmatrix} -H_2^H \mathbf{c}_M \\ \mathbf{0}_{(N-k_2) \times 1} \end{bmatrix} \quad (21)$$

where  $(\cdot)^H$  stands for the conjugate transpose operation,  $I_M$  is the  $M \times M$  identity matrix,  $\mathbf{e}_{M+k_1} = [0 \ \dots \ 0 \ 1]^T$  and the  $M \times (k_1 + M)$ ,  $M \times k_2$  matrices  $H_1$ ,  $H_2$  are given as shown in (22) and (23), at the bottom of the next page. It is shown in the Appendix, that for the special class of channels we consider, and for medium or high SNRs, the solution of (20) can be approximated very closely by the solution of the much more simple set of equations

$$H_{12}^H \hat{\mathbf{c}}_M = \mathbf{e}_M \quad (24)$$

where  $\mathbf{e}_M = [0 \ \dots \ 0 \ 1]^T$ . Obviously, to solve the above system the condition that the  $M \times M$  matrix  $H_{12}^H$  is nonsingular is required.

1) *Solution of  $H_{12}^H \hat{\mathbf{c}}_M = \mathbf{e}_M$ :* From (22),  $H_{12}^H$  can be written as

$$H_{12}^H = h_0^* I_M + F = h_0^* (I_M + h_0^{*-1} F) \quad (25)$$

<sup>5</sup>Equations (20) and (21) can be derived by extending in matrix form and for the noncausal channel case [1, eqs. (10-3-3), (10-3-4), and (10-3-5)]. An alternative derivation can be found in [21].

where  $F$  results from  $H_{12}^H$  after removing its main diagonal, i.e.,

$$F = \begin{bmatrix} 0 & h_{-1}^* & \cdots & h_{-k_1}^* & \cdots & 0 \\ h_1^* & 0 & \cdots & h_{-k_1+1}^* & \cdots & \vdots \\ \vdots & \vdots & \vdots & \vdots & \vdots & h_{-k_1}^* \\ \vdots & \vdots & \vdots & \vdots & \vdots & \vdots \\ h_{M-2}^* & h_{M-3}^* & \cdots & \cdots & \cdots & h_{-1}^* \\ h_{M-1}^* & h_{M-2}^* & \cdots & \cdots & h_1^* & 0 \end{bmatrix}. \quad (26)$$

By assuming that  $\|F\| < |h_0|$ , where  $\|\cdot\|$  stands for any matrix norm, we can express  $\hat{\mathbf{c}}_M$  by means of a Taylor series expansion as follows<sup>6</sup>:

$$\hat{\mathbf{c}}_M = (H_{12}^H)^{-1} \mathbf{e}_M \approx h_0^{*-1} (I_M - h_0^{*-1} F + h_0^{*-2} F^2) \mathbf{e}_M \quad (27)$$

where up to second-order terms have been kept in the expansion. Due to the sparseness of the channel IR and the form of matrix  $F$ ,  $\hat{\mathbf{c}}_M$  can be directly expressed in terms of the nonzero coefficients of the channel IR. More specifically, from (27) and the definition of  $\mathbf{e}_M$ , we easily derive the following results concerning zeroth-, first-, and second-order terms of  $\hat{\mathbf{c}}_M$ , respectively.

- There exists a zeroth-order contribution, equal to  $h_0^{*-1}$ , to the last element of  $\hat{\mathbf{c}}_M$ .
- For each  $n_i < 0$ , there is a first-order contribution, equal to  $-h_0^{*-2} h_{n_i}^*$ , to the  $(M + n_i)$ th element of  $\hat{\mathbf{c}}_M$ . This is obvious if we see that  $F\mathbf{e}_M$  is in fact the last column of  $F$ .
- For each combination of  $n_i, n_j$  with  $n_i + n_j < 0$  there is a second-order contribution, equal to  $h_0^{*-3} h_{n_i}^* h_{n_j}^*$ , to the  $(M + n_i + n_j)$ th element of  $\hat{\mathbf{c}}_M$ . This is shown by forming the product of  $F$  with its last column  $F\mathbf{e}_M$  and taking into account the positions of the nonzero elements of the channel IR.

<sup>6</sup>If, for instance,  $\|\cdot\|$  denotes the row matrix norm, this assumption requires that the maximum sum of amplitudes of any  $M$  consecutive channel IR coefficients,  $h_i$ , with  $i$  in the range  $-k_1$  to  $M$ ,  $i \neq 0$ , is less than  $|h_0|$ . Such a condition seems to be realistic in the applications of interest, e.g., it is easily met in all test channels of [17].

In conclusion, vector  $\hat{\mathbf{c}}_M$  can be expressed up to second-order approximation as follows:

$$\hat{\mathbf{c}}_M \approx h_0^{*-1} \mathbf{e}_M^{(M)} - h_0^{*-2} \sum_{n_i < 0} h_{n_i}^* \mathbf{e}_M^{(M+n_i)} + h_0^{*-3} \sum_{n_i + n_j < 0} \sum h_{n_i}^* h_{n_j}^* \mathbf{e}_M^{(M+n_i+n_j)} \quad (28)$$

where  $\mathbf{e}_M^{(k)} = [0 \ \cdots \ 0 \ 1 \ 0 \ \cdots \ 0]^T$  of length  $M$  has one in its  $k$ th position. Following the analysis of the Appendix, we deduce that the FF filter  $\mathbf{c}_M$ , computed exactly via (20), can also be expressed by (28) with a very high degree of precision.

2) *The FB filter  $\mathbf{b}_N$* : The form of the FB filter  $\mathbf{b}_N$  can be now obtained by combining (21), (23), and (28). More specifically, from (23) and (28) and the result of the Appendix, we get

$$H_2^H \mathbf{c}_M \approx h_0^{*-1} \mathbf{h}_2^{(M)} - h_0^{*-2} \sum_{n_i < 0} h_{n_i}^* \mathbf{h}_2^{(M+n_i)} + h_0^{*-3} \sum_{n_i + n_j < 0} \sum h_{n_i}^* h_{n_j}^* \mathbf{h}_2^{(M+n_i+n_j)} \quad (29)$$

where  $\mathbf{h}_2^{(k)}$  stands for the  $k$ th column of  $H_2^H$ . Since for each  $l$  with  $n_l > 0$ ,  $h_{n_l}^*$  is the  $n_l$ th element of the last column of  $H_2^H$  and matrix  $H_2^H$  has a Toeplitz form, we deduce from (21) and (29) that the FB filter possesses approximately the following structure.

- 1) There are first-order (“primary”) nonzero taps at the positions  $n_l$  where  $n_l > 0$  is a position of a causal component in the channel IR.
- 2) For each “primary” tap at  $n_l > 0$ , there are second-order nonzero taps at the positions  $n_l + n_i > 0$ , where  $n_i < 0$  are positions of the anticausal components in the channel IR.
- 3) For each “primary” nonzero tap at  $n_l > 0$ , there are third-order terms located at  $n_l + n_i + n_j > 0$ , where  $n_i, n_j$  is any combination of component locations with  $n_i + n_j < 0$ .

Thus, it turns out that the FB filter has a sparse form and, hence, can be restricted to act to the above positions only. In case strong

$$H_1 \equiv [H_{11} \mid H_{12}] = \left[ \begin{array}{cccc|cccccc} h_{-k_1} & h_{-k_1+1} & \cdots & h_{-1} & h_0 & h_1 & \cdots & \cdots & h_{M-2} & h_{M-1} \\ 0 & h_{-k_1} & \cdots & h_{-2} & h_{-1} & h_0 & \cdots & \cdots & h_{M-3} & h_{M-2} \\ \vdots & \vdots \\ 0 & 0 & \cdots & h_{-k_1} & h_{-k_1+1} & \cdots & \cdots & \cdots & \cdots & h_{M-k_1} \\ \vdots & \vdots \\ 0 & 0 & \cdots & 0 & 0 & \cdots & h_{-k_1} & \cdots & h_{-1} & h_0 \end{array} \right] \quad (22)$$

$$H_2 = \left[ \begin{array}{cccc|cc} h_M & h_{M+1} & \cdots & h_{k_2} & 0 & \cdots & 0 \\ h_{M-1} & h_M & \cdots & \cdots & h_{k_2} & \cdots & 0 \\ \vdots & \vdots & \vdots & \vdots & \vdots & \vdots & \vdots \\ h_1 & h_2 & \cdots & \cdots & \cdots & \cdots & h_{k_2} \end{array} \right] \quad (23)$$

TABLE I  
BASIC STEPS OF THE SPARSE DFE (SDFE) ALGORITHM

1. Compute $C_{UX}^{(R)}(k)$ from (17).
2. Compute the IDFT of $C_{UX}^{(R)}(k)$ .
3. Estimate the locations of the channel IR components based on a threshold (section III)
4. Identify the primary and secondary FB tap positions (section IV-A)
5. For the next $N$ iterations, apply the DFE with the FB filter acting to the above positions.
6. Update $C_{UX}^{(R)}(k)$ from (19) and repeat from step 2.

TABLE II  
COMPARISON IN TERMS OF THE NUMBER OF COMPLEX MULTIPLICATIONS

Conventional DFE	$2M + 2N$
SDFE-(2)	$2M + 3\log_2(N) + 2L_1(L_2 + 1) + 5$
SDFE-(3)	$2M + 3\log_2(N) + 2L_1(L_2 + S + 1) + 5$

echoes are not present in the channel IR, a second-order approximation of the FB filter [points 1) and 2) above] seems to be sufficient for the proposed algorithm to achieve a performance similar to that of the conventional DFE. However, when there are strong components in the channel IR (especially strong precursor components), a higher number of taps should be considered for the FB filter as dictated by point 3). This results in a slight increase of the computational complexity of the proposed algorithm. In any case, the FB filter comprises a small number of taps and the novel sparse equalizer offers considerable computational savings compared with the conventional DFE, as demonstrated in the next section. The basic steps of the proposed sparse DFE (SDFE) algorithm are summarized in Table I.

### B. Complexity Issues

The main feature of the algorithm described in Section IV-A is that instead of a long FB filter, it uses a small number of nonzero FB taps. As a result, it is expected that its computational load will be equally reduced compared with the conventional DFE structure. In Table II, the computational complexity (expressed in number of complex multiplications per sample) of the proposed algorithm is compared with that of the conventional DFE, under the assumption that  $N$  is a power of two. Both cases of a second [SDFE-(2)] and a third [SDFE-(3)] order approximation of the FB filter are considered as analyzed in Section IV-A2. In Table II,  $L_1$ ,  $L_2$  correspond to the number of detected causal and noncausal multipath components, respectively.  $S$  stands for the number of pairs of locations  $n_i$ ,  $n_j$  for which  $n_i + n_j < 0$ . It can be verified that both variations of the new DFE have significantly lower computational complexity compared with that of the conventional DFE. This is so because the complexity of the conventional algorithm depends linearly on  $N$ , while the complexity of the proposed algorithm depends on  $\log_2(N)$ . The reduction in the computational load achieved by the new schemes is better illustrated in Table III. In

TABLE III  
NUMBER OF COMPLEX MULTIPLICATIONS FOR CERTAIN SPECIFICATIONS

Specifications					Algorithms		
$M$	$N$	$L_1$	$L_2$	$S$	DFE	SDFE-(2)	SDFE-(3)
30	128	6	2	4	316	122	170
30	256	7	2	4	572	131	187
60	256	7	3	5	632	205	275
60	512	8	3	6	1144	216	312

this table, the number of complex multiplications required by DFE, SDFE-(2), and SDFE-(3) is calculated for certain specifications. Observe that in a typical case encountered in HDTV ( $M = 30$ ,  $N = 256$ ) a reduction of more than 70% in the number of complex multiplications is attained. Similar complexity improvements are also achieved for all other cases considered in Table III.

## V. SIMULATION RESULTS

The new DFE algorithms have been extensively tested for different sparse channels (including measured microwave channels) and various input and noise specifications. Their performance has been evaluated not only under time invariant conditions, but also in a time-varying environment. Some simulation results are described below.

Fig. 1 shows a typical terrestrial HDTV channel IR. The channel IR is the convolution of test channel D of [17] with a square-root raised cosine filter with 11.5% rolloff. Note the presence of four postcursor components, including a strong far echo, and one precursor component of relatively low magnitude. The input to the channel is a 16-quadrature amplitude modulation (QAM) sequence, while complex white Gaussian noise is added to the channel output resulting in an SNR of 25 dB.

The magnitude of the MMSE FB filter taps, which correspond to the channel IR of Fig. 1, is shown in Fig. 2(a). The FB filter taps are calculated directly from (20) and (21). We observe that besides the dominant nonzero taps which correspond to the causal components of the channel IR, there exist secondary taps equally spaced from the dominant ones. The “distance” between dominant and secondary taps equals to the “distance” of the precursor component from the main signal in the channel IR. We see from Fig. 2(a) that all other taps can be considered negligible.

The magnitude of the MMSE FB filter taps for a channel IR with a strong precursor component is shown in Fig. 2(b). Specifically, in the sparse channel of Fig. 1, we increase the amplitude of the precursor component from 0.1 to 0.4. We see that the sparseness of the FB filter has decreased, however, the positions of the significant nonzero taps are still in accordance with those estimated from our method using higher than second-order approximation.

In Fig. 3(a), the performance of the new technique is compared with that of the conventional DFE, for the channel IR of Fig. 1, when a training sequence of 640 symbols is used. Note

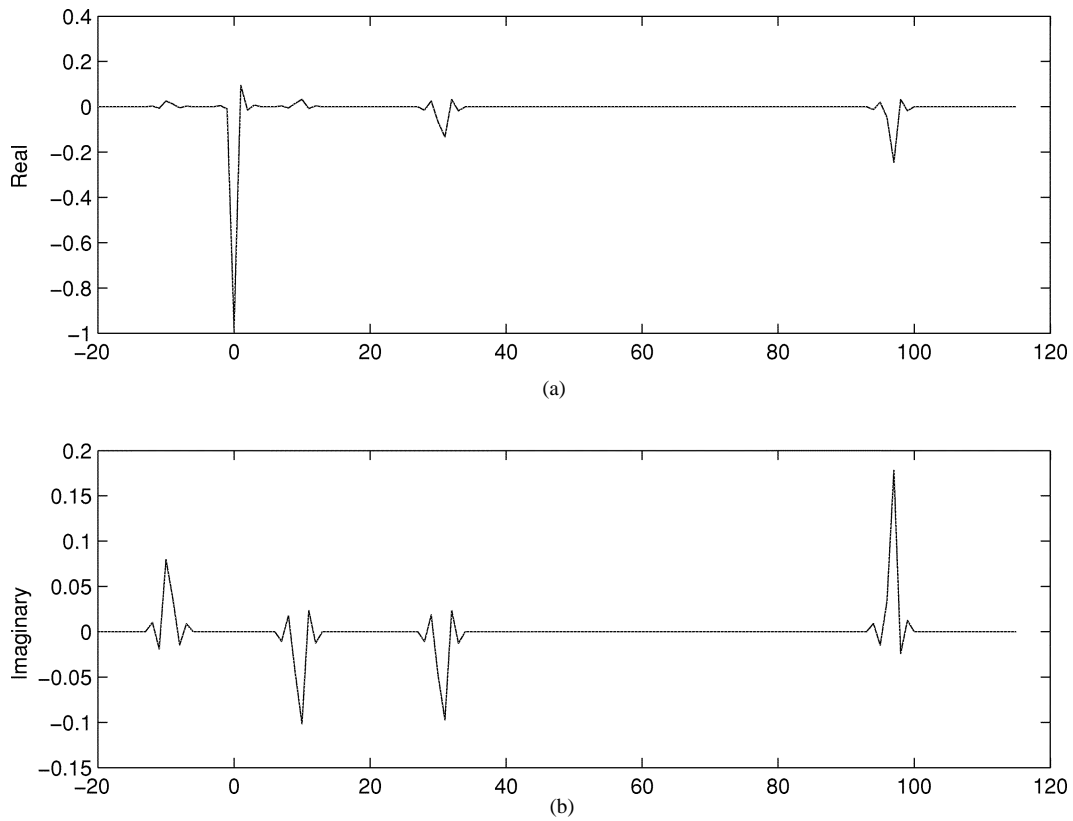


Fig. 1. Multipath channel impulse response.

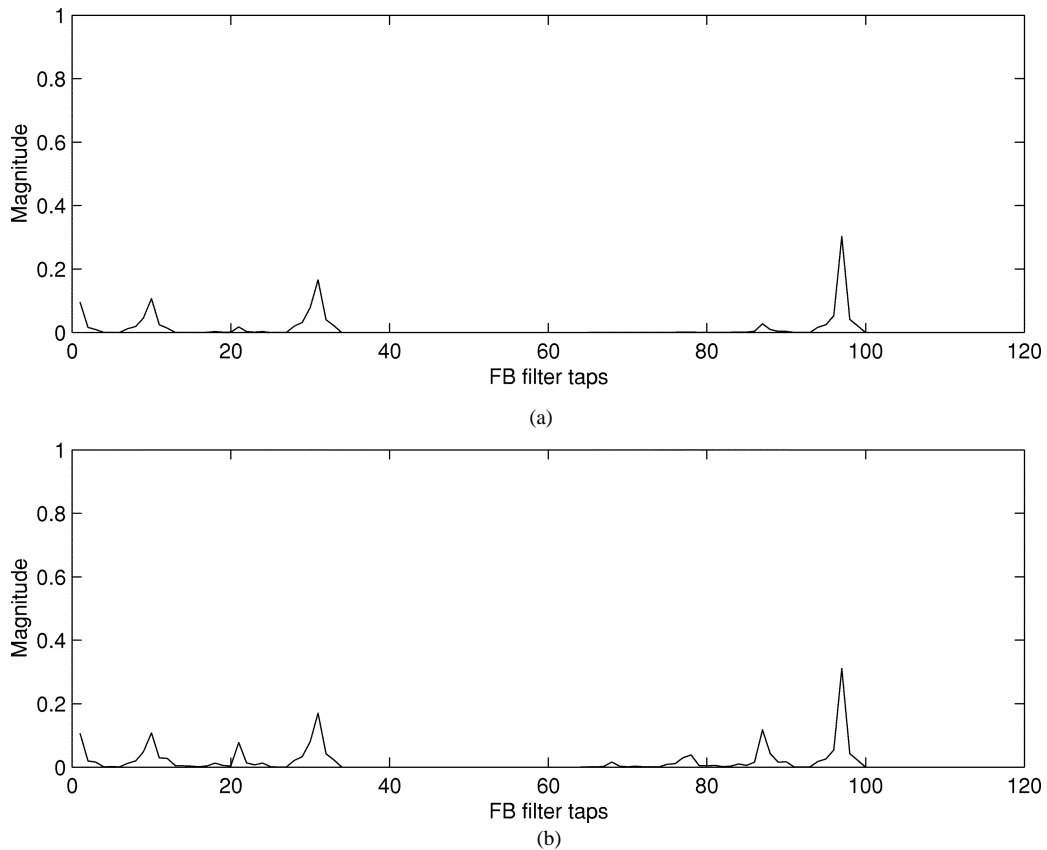


Fig. 2. MMSE FB filter coefficients (a) for the channel IR of Fig. 1 and (b) when a strong precursor echo is present.

that the length of the training sequence is short relative to the channel IR span. Two MSE curves are depicted in Fig. 3(a).

The solid line curve corresponds to the conventional DFE with  $M = 30$ ,  $N = 128$ , and the dotted curve to the proposed

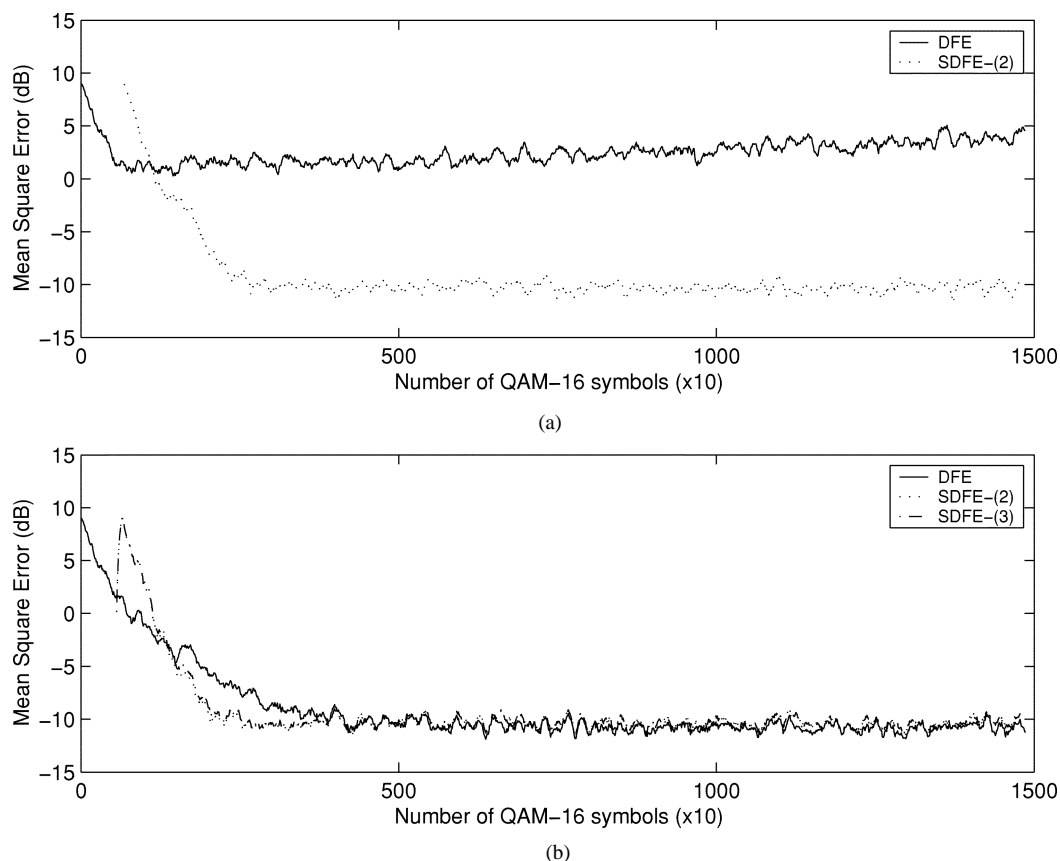


Fig. 3. (a) Initial convergence MSE curves of DFE and SDFE for the channel IR of Fig. 1. (b) Steady-state MSE curves of DFE and SDFE for the channel IR of Fig. 1.

algorithm with second-order approximation of the FB filter. The number of multipath components has been preset to 8 and  $\lambda = 1$ . Note that the FB tap reduction achieved by the new algorithm is of the order of 78%. We observe that due to the small size of the training sequence, the DFE algorithm fails to converge to the steady state. On the other hand, the number of training symbols is sufficient for the SDFE-(2) algorithm not only to detect the component locations, but also to converge to the steady state.

In the sequel, we increase the number of training symbols in order to compare the steady-state error performance of the algorithms under consideration. Three MSE curves are shown in Fig. 3(b). The solid line curve corresponds to the conventional DFE and the dotted and dashed curves to the proposed algorithm with second- and third-order approximation of the FB filter. We see that all three DFEs have similar steady-state performance, i.e., a second-order approximation of the FB filter seems to be sufficient. However, despite their initial delay required for the detection of the time delays, the new algorithms converge to the steady-state faster than the conventional DFE. This fact is fully justified by the existence of a reduced size FB filter in the structure of the new algorithm, meaning that its convergence rate is mainly governed by the FB filter size. On the other hand, the long FB filter of the conventional DFE slows down significantly its initial convergence.

Fig. 4 shows how the steady-state error performance is affected by the presence of a strong precursor echo in the channel IR. The MSE curves of Fig. 4(a) verify that there is

a slight steady-state performance degradation of the proposed DFE, when a second-order approximation of the FB filter is used. However, when third-order FB terms are taken into consideration, the performance of the new algorithm becomes almost similar to that of the conventional DFE, as illustrated in Fig. 4(b). Note that the FB tap reduction is of the order of 78% and 74%, when second- and third-order approximation is used, respectively.

Fig. 5 shows the symbol-error rate (SER) of the proposed and the conventional DFE algorithms, under different SNR, when a strong precursor echo is present. This figure demonstrates the slight increase of the new algorithm's SER when only up to second-order FB taps are taken into consideration, as well as its performance improvement, when a slightly higher number of taps are used by the FB filter.

In order to investigate the tracking ability of the new algorithm in a time-varying environment, we consider the following scenario. After 6000 iterations, the phases of the second and third postcursor components of the channel of Fig. 1 start continuously rotating, while their amplitudes are kept fixed. The phases' rotation step is  $2\pi(0.02/360)$  rad per iteration. The MSE of the SDFE algorithm with a forgetting factor  $\lambda = 0.999$  is compared with that of the conventional DFE in Fig. 6. We see that the proposed algorithm immediately tracks the change in the environment and as a result the misadjustment error is small. On the contrary, the long FB filter of the conventional algorithm drastically affects its tracking ability, resulting in a high misadjustment error. The proposed algorithm has also been

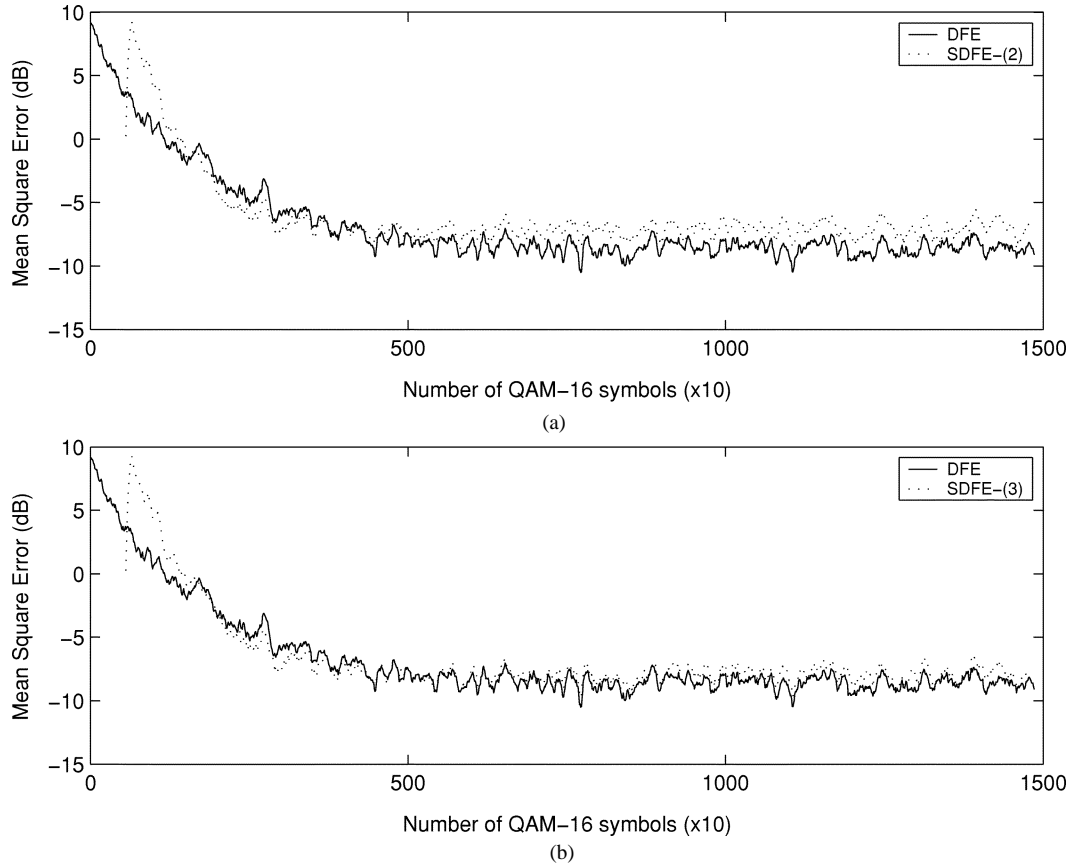


Fig. 4. MSE curves for (a) DFE and SDFE-(2) and (b) DFE and SDFE-(3) when a strong precursor echo is present.

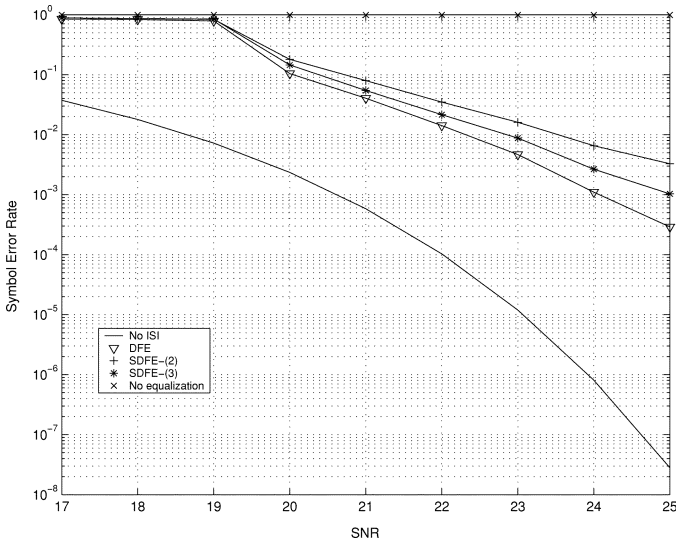


Fig. 5. SER curves for DFE, SDFE-(2) and SDFE-(3) when a strong precursor echo is present.

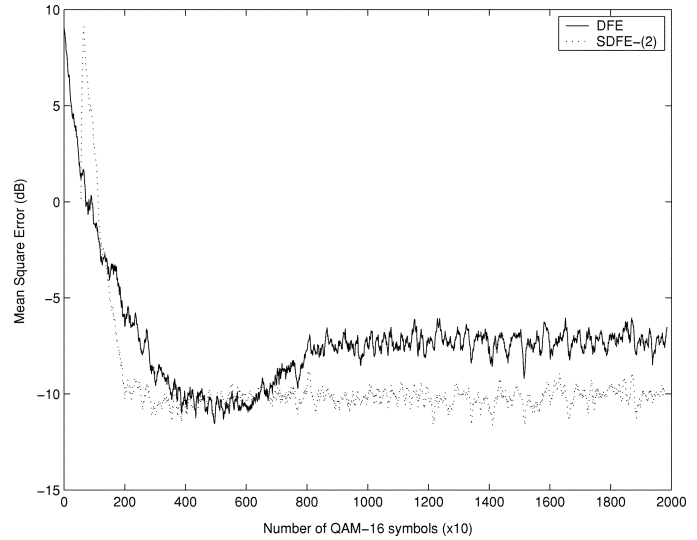


Fig. 6. MSE curves under time-varying conditions.

tested for other time-varying situations, e.g., when one or more echoes appear in or disappear from the channel IR. In all experiments carried out, the new DFE exhibited a superior performance in terms of tracking compared with the conventional algorithm.

We complete our simulation tests by examining the performance of the new algorithm for a measured microwave channel

IR. This channel IR corresponds to *chan15.mat* that is taken from the Rice University Signal Processing Information Base (SPIB).<sup>7</sup> Its magnitude is plotted in Fig. 7(a). The magnitude of the corresponding MMSE FB filter coefficients with an SNR = 25 dB is shown in Fig. 7(b). It is clear that the FB filter has a sparse form and the locations of the significant nonzero FB

<sup>7</sup>*chan15.mat* can be found at the URL, <http://spib.rice.edu/spib/microwave.html>

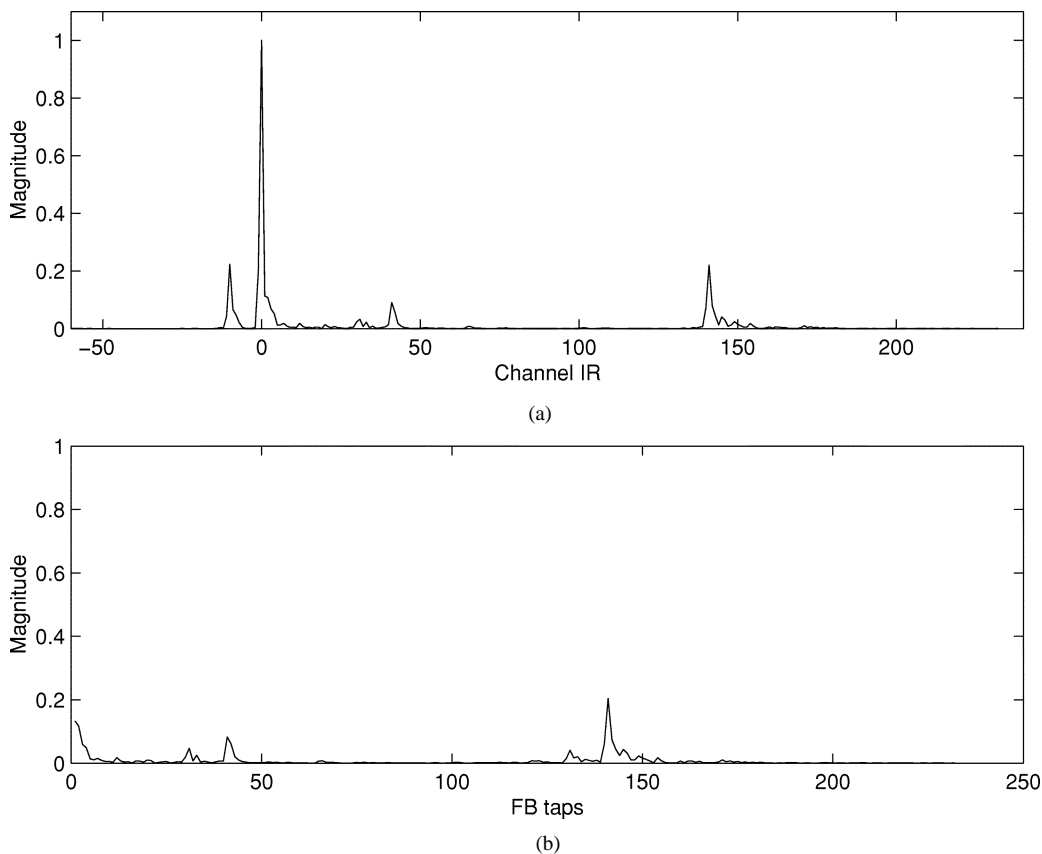


Fig. 7. (a) Magnitude of the microwave channel IR. (b) Magnitude of the MMSE FB coefficients for the microwave channel IR.

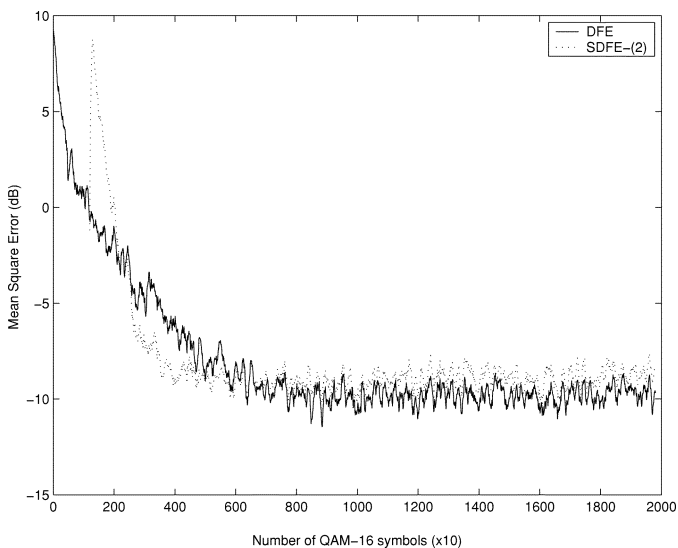


Fig. 8. MSE curves of DFE and SDFE-(2) for the measured microwave channel IR.

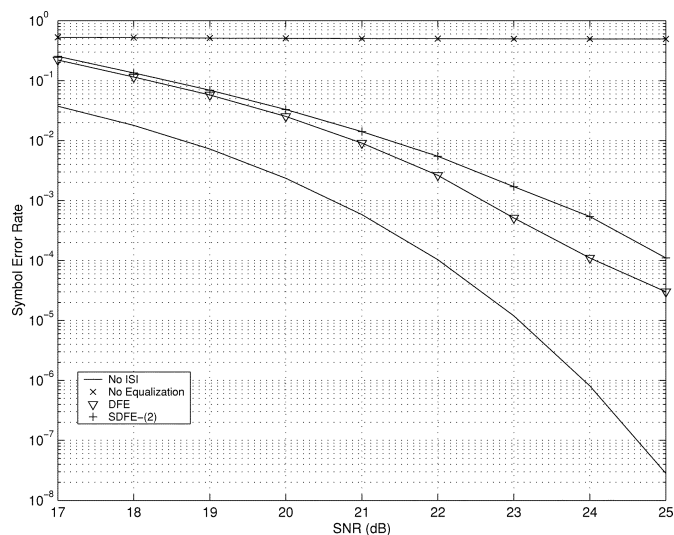


Fig. 9. SER curves for the measured microwave channel IR.

taps are in agreement with those estimated using our method. In Fig. 8, the MSE of the DFE with  $M = 40$ ,  $N = 256$  is compared with the MSE of the SDFE-(2) algorithm with a 78% FB tap reduction. We see that our approach provides faster initial convergence and its steady-state error is very close to that of the conventional algorithm. Finally, the curves of Fig. 9 verify that the SER of the proposed algorithm is very close to that of the classical DFE, although the new method uses less than one fourth of the FB taps of the conventional algorithm.

## VI. CONCLUSION

In this paper, the sparse form encountered in many high-speed wireless communications channels is properly exploited in two ways. First, the time delays of the dominant multipath components are efficiently estimated and continuously updated using a frequency domain approach. Second, an approximate form of the FB filter of the MMSE-DFE is derived. Based on the above, a new efficient DFE algorithm is proposed, whose FB filter comprises a reduced number of active taps. Depending on

the multipath channel conditions, there may exist a tradeoff between the number of FB taps used and the performance of the proposed algorithm. In general, the new algorithm offers considerable computational savings, faster convergence, and better tracking capabilities while exhibiting almost identical steady-state performance in most practical cases, as compared with the conventional DFE. The features of the new algorithm have been confirmed through extensive simulation tests.

#### APPENDIX

To start with, we ignore noise and examine its contribution at the end of the appendix. Now, if we ignore the term  $(\sigma_w^2/\sigma_u^2)I_M$ , (20) can be interpreted as the solution of a least squares (LS) problem with data matrix equal to  $H_1^H$  and desired response vector equal to  $\mathbf{e}_{M+k_1}$ . Similarly,  $\hat{\mathbf{c}}_M$  in (24) is in fact the solution of a LS problem with data matrix  $H_{12}^H$  and desired response vector  $\mathbf{e}_M$ . Since  $H_{12}^H$  is the lower  $M \times M$  part of  $H_1^H$  and  $\mathbf{e}_M$  is the lower  $M \times 1$  part of  $\mathbf{e}_{M+k_1}$ , the solution of the former LS problem can be reached by the solution of the latter problem by following a recursive LS (RLS) procedure [20]. This procedure consists of  $k_1$  update steps, one step for each row of the matrix  $H_{11}^H$ . The first update step of this procedure is described by the following pair of equations

$$v(1) = -\mathbf{h}^H(1)\hat{\mathbf{c}}_M(0) \quad (30)$$

$$\hat{\mathbf{c}}_M(1) = \hat{\mathbf{c}}_M(0) + (H_{12}(1)H_{12}^H(1))^{-1} \mathbf{h}(1)v(1) \quad (31)$$

where  $\hat{\mathbf{c}}_M(0) \equiv \hat{\mathbf{c}}_M$ ,  $v(1)$  is the LS estimation error,  $H_{12}^H(1)$  is the lower  $(M+1) \times M$  block of matrix  $H_1^H$ , and  $\mathbf{h}^T(1) = [h_{-1}^* \ \dots \ h_{-k_1}^* \ 0 \ \dots \ 0]$  is the last row of  $H_{11}^H$ . Let us now examine how the LS solution is affected by the first update step. To this end, we form the following norm:

$$\begin{aligned} \|\hat{\mathbf{c}}_M(1) - \hat{\mathbf{c}}_M(0)\| &= \left\| (H_{12}(1)H_{12}^H(1))^{-1} \mathbf{h}(1)v(1) \right\| \\ &\leq \left\| (H_{12}(1)H_{12}^H(1))^{-1} \right\| \cdot \|\mathbf{h}(1)\| \cdot |v(1)| \end{aligned} \quad (32)$$

where  $\|\cdot\|$  stands for any typical matrix norm. To proceed further, we make the following assumptions.

*Assumption 1:*  $M \geq 3k_1$ . Commonly, the FF filter length must be several times larger than the anticausal part [14].

*Assumption 2:*  $|h_0|$  is  $O(1)$  and  $|h_{n_i}|$  is  $O(\varepsilon)$  for  $n_i \neq 0$ , where  $\varepsilon$  is a small positive real number with  $0 < \varepsilon < 1$ . This assumption also holds true for the channels of interest as discussed so far. Of course the less than one is  $\varepsilon$  the higher the accuracy of our approximation becomes.

*Assumption 3:*  $M$  is  $O(\varepsilon^{-2})$  and  $k_1$  is  $O(\varepsilon^{-1})$ . This assumption is an outcome of the previous two.

Based on the above assumptions, an estimation of the order of each term in the right-hand side (RHS) of (32), as a function of  $\varepsilon$ , will be obtained. Specifically, the following.

- 1)  $\|\mathbf{h}(1)\|$  is  $O(\varepsilon)$ .
- 2) Since  $M \geq 3k_1$  and the upper  $k_1 \times 1$  part of  $\hat{\mathbf{c}}_M(0)$  contains higher than second-order terms, we easily deduce from (30) and the form of  $\mathbf{h}(1)$  that  $|v(1)|$  is  $O(\varepsilon^4)$ .

3) The term  $\|(H_{12}(1)H_{12}^H(1))^{-1}\|$  can be expressed as

$$\|(H_{12}(1)H_{12}^H(1))^{-1}\| = \frac{\text{cond}(H_{12}(1)H_{12}^H(1))}{\|H_{12}(1)H_{12}^H(1)\|} \quad (33)$$

for any matrix norm  $\|\cdot\|$ , where  $\text{cond}(\cdot)$  denotes the condition number of a matrix. If  $\|\cdot\|$  stands for the row matrix norm, we see from (22) that  $\|H_{12}(1)H_{12}^H(1)\|$  is at least  $O(1)$ . What now remains is to evaluate the quantity  $\text{cond}(H_{12}(1)H_{12}^H(1))$ . This quantity can be alternatively written as follows:

$$\text{cond}(H_{12}(1)H_{12}^H(1)) = \frac{\lambda_{\max}(H_{12}(1)H_{12}^H(1))}{\lambda_{\min}(H_{12}(1)H_{12}^H(1))} \quad (34)$$

where  $\lambda_{\max}(\cdot)$ ,  $\lambda_{\min}(\cdot)$  are the maximum and minimum eigenvalues of a matrix, respectively. Moreover, matrix  $H_{12}(1)H_{12}^H(1)$  can be written as

$$H_{12}(1)H_{12}^H(1) = |h_0|^2 I_M + A \quad (35)$$

where the  $M \times M$  matrix  $A$  results from  $H_{12}(1)H_{12}^H(1)$  after subtracting the quantity  $|h_0|^2$  from each diagonal element. Combining (34) and (35), we get

$$\text{cond}(H_{12}(1)H_{12}^H(1)) = \frac{|h_0|^2 + \lambda_{\max}(A)}{|h_0|^2 + \lambda_{\min}(A)}. \quad (36)$$

From (36), it is readily understood that in order for matrix  $H_{12}(1)H_{12}^H(1)$  to be well conditioned, it suffices to show that  $\lambda_{\max}(A)$  is bounded by a relatively small number. Note that  $A$  is hermitian symmetric and nonnegative definite, therefore, it has nonnegative eigenvalues and moreover it holds  $\lambda(AA^H) = \lambda^2(A)$  for any eigenvalue of  $A$ . Consequently, we have [22]

$$\|A\|_{\text{spec}} = \sqrt{\lambda_{\max}(AA^H)} = \lambda_{\max}(A) \quad (37)$$

where  $\|A\|_{\text{spec}}$  stands for the spectral norm of  $A$  [22]. Moreover [22]

$$\|A\|_{\text{spec}} \leq M\|A\|_{\infty} \quad (38)$$

where  $\|A\|_{\infty} = \{\max |a_{ij}|, i, j = 1, 2, \dots, M\}$ . From (37) and (38), we are led to the inequality

$$\lambda_{\max}(A) \leq M \max |a_{ij}|. \quad (39)$$

From the form of  $A$ , it is easily seen that its maximum element is  $O(\varepsilon)$ . Based on assumption 3 and (39), we then deduce that  $\lambda_{\max}(A)$  is bounded by a number which is  $O(\varepsilon^{-1})$ . From (36) and (33), we see that the same also holds for the quantity  $\|(H_{12}(1)H_{12}^H(1))^{-1}\|$ .

If we now combine the results of points 1, 2, and 3 above, we derive that the norm in the left-hand side of (32) is bounded by a number which is  $O(\varepsilon^4)$ . By repeating the same procedure for the remaining  $k_1 - 1$  update steps, we end up with the following result:

$$\|\hat{\mathbf{c}}_M(k_1) - \hat{\mathbf{c}}_M(0)\|_2 \leq \varrho \quad (40)$$

where  $\varrho$  is  $O(\varepsilon^3)$ , due to assumption 3.

In conclusion, in the noise free case, the difference between the exact LS solution and the approximated one can be considered negligible. The contribution of noise in (20) can be interpreted as a perturbation to the associated system matrix affecting the solution  $\hat{c}_M(k_1)$ . It can be easily shown, by using well-known results concerning bounds on the accuracy of perturbed linear systems solutions [22], that for medium or high SNR the perturbation error is bounded by  $(\sigma_w^2/\sigma_u^2)\xi$ , where  $\xi$  is an  $O(\varepsilon^{-1})$  quantity.

REFERENCES

[1] J. G. Proakis, *Digital Communications*, 3rd ed. New York: McGraw-Hill, 1995.

[2] T. S. Rappaport, *Wireless Communications: Principles and Practice*. Englewood Cliffs, NJ: Prentice-Hall, 1996.

[3] J. Salz, "Optimum mean-square decision feedback equalization," *Bell Syst. Tech. J.*, vol. 52, no. 8, pp. 1341–1373, Oct. 1973.

[4] G. Young, "Reduced complexity decision feedback equalization for digital subscriber loops," *IEEE J. Select. Areas Commun.*, vol. 9, pp. 810–816, Aug. 1991.

[5] P. Crespo and M. Honig, "Pole-zero decision feedback equalization with a rapidly converging adaptive IIR algorithm," *IEEE J. Select. Areas Commun.*, vol. 9, pp. 817–829, Aug. 1991.

[6] N. Al-Dhahir and J. M. Cioffi, "Stable pole-zero modeling of long FIR filters with application to the MMSE-DFE," *IEEE Trans. Commun.*, vol. 45, pp. 508–513, May 1997.

[7] K. Berberidis and J. Palicot, "A frequency-domain DFE for multipath echo cancellation," in *Proc. IEEE GLOBECOM*, Singapore, Nov. 1995, pp. 98–102.

[8] K. Berberidis, T. A. Rontogiannis, and S. Theodoridis, "Efficient block implementation of the DFE," *IEEE Signal Processing Lett.*, vol. 5, pp. 129–131, June 1998.

[9] K. Berberidis and P. Karaivazoglou, "A block adaptive DFE in the frequency domain based on tentative decisions," in *Proc. EUSIPCO*, Rodos, Sept. 1998.

[10] N. Al-Dhahir and J. M. Cioffi, "Fast computation of channel-estimate based equalizers in packet data transmission," *IEEE Trans. Signal Processing*, vol. 43, pp. 2462–2473, Nov. 1995.

[11] S. Ariyavisitakul and L. J. Greenstein, "Reduced-complexity equalization techniques for broadband wireless channels," *IEEE J. Select. Areas Commun.*, vol. 15, pp. 5–15, Jan. 1997.

[12] R. Gupta, Kiran, and E. Lee, "Computationally efficient version of the decision feedback equalizer," in *Proc. IEEE ICASSP*, Seattle, 1999, pp. 1257–1260.

[13] S. Ariyavisitakul, N. R. Sollenberger, and L. J. Greenstein, "Tap-selectable decision feedback equalization," *IEEE Trans. Commun.*, vol. 45, pp. 1498–1500, Dec. 1997.

[14] I. J. Fevrier, S. B. Gelfand, and M. P. Fitz, "Reduced complexity decision feedback equalization for multipath channels with large delay spreads," *IEEE Trans. Commun.*, vol. 47, pp. 927–937, 1999.

[15] S. F. Cotter and B. D. Rao, "Matching pursuit based decision-feedback equalizers," in *Proc. IEEE ICASSP*, Istanbul, Turkey, June 2000.

[16] K. Berberidis and A. A. Rontogiannis, "Efficient decision feedback equalizer for sparse multipath channels," in *Proc. IEEE ICASSP*, Istanbul, Turkey, June 2000.

[17] M. Ghosh, "Blind decision feedback equalization for terrestrial television receivers," *Proc. IEEE*, vol. 86, pp. 2070–2081, Oct. 1998.

[18] I. Kang, M. P. Fitz, and S. B. Gelfand, "Blind estimation of multipath channels: A modal analysis approach," *IEEE Trans. Commun.*, vol. 47, pp. 1140–1150, Aug. 1999.

[19] A. A. Rontogiannis, A. Marava, K. Berberidis, and J. Palicot, "Semi-blind estimation of multipath channel parameters via a separable least squares approach," in *Proc. 14th Digital Signal Processing Conf.*, Santorini, July 2002, pp. 49–52.

[20] M. H. Hayes, *Statistical Digital Signal Processing and Modeling*. New York: Wiley, 1996.

[21] K. Berberidis, A. Marava, P. Karaivazoglou, and J. Palicot, "Robust and fast converging decision feedback equalizer based on a new adaptive semi-blind channel estimation algorithm," in *Proc. IEEE GLOBECOM*, San Antonio, TX, 2001, pp. 269–273.

[22] R. A. Horn and C. R. Johnson, *Matrix Analysis*. Cambridge, U.K.: Cambridge Univ. Press, 1999.



**Athanasios A. Rontogiannis** (SM'92–M'98) was born in Lefkada, Greece, in 1968. He received the Diploma in electrical engineering from the National Technical University of Athens, Greece, the M.A.Sc. degree from the University of Victoria, BC, Canada, and the Ph.D. degree in communications and signal processing from the University of Athens, Greece, in 1991, 1993, and 1997, respectively.

From March 1997 to November 1998, he served his military service with the Greek Air Force. In November 1998, he joined the School of Natural Resources and Enterprises Management, University of Ioannina, Greece, where he is a Lecturer in Informatics since June 2000. His research interests are in the areas of adaptive signal processing and signal processing for communications.

Dr. Rontogiannis is a Member of the Technical Chamber of Greece.



**Kostas Berberidis** (S'87–M'90) was born in Serres, Greece, in 1962. He received the Diploma degree in electrical engineering from the Democritus University of Thrace, Greece, in 1985 and the Ph.D. degree in computer engineering and informatics from the University of Patras, Greece, in 1990.

From 1986 to 1990, he was a Research Assistant at the Computer Technology Institute (C.T.I.), Patras, Greece and a Teaching Assistant at the Computer Engineering and Informatics Department, University of Patras. During 1991, he served in the Greek Army working at the Speech Processing Lab of the National Defense Research Center. From 1992 to 1994 and from 1996 to 1997, he was a Researcher at the Research and Development Department of C.T.I. During the academic year 1994/1995, he was a Postdoctoral Fellow at the Centre Commun d'Etudes de Telediffusion et Telecommunications (C.C.E.T.T.), Rennes, France. Since December 1997, he has been with the Department of Computer Engineering and Informatics, School of Engineering, University of Patras, where he is currently an Assistant Professor and Head of the Signal Processing and Communications Lab. His research interests include digital signal processing, adaptive filtering, and digital communications.

Dr. Berberidis is a Member of the Technical Chamber of Greece.